Published in final edited form as:

Adv Funct Mater. 2021 February 3; 31(6): . doi:10.1002/adfm.202003341.

Macrophage immunomodulation through new polymers that recapitulate functional effects of itaconate as a power house of innate immunity

L. Davenport Huyer[1,2,3], **S. Mandla**[2,3], **Y. Wang**[1,3], **S. Campbell**[2,3], **B. Yee**[1,3], **C. Euler**[1], **B. F. Lai**[2], **D. Bannerman**[1,2,3], **D. S. Y. Lin**[2], **M. Montgomery**[1,2,3], **K. Nemr**[1], **T. Bender**[1], **S. Epelman**[3], **R. Mahadevan**[1,2], **M. Radisic**[1,2,3,*]

[1]Department of Chemical Engineering and Applied Chemistry, University of Toronto, Toronto, Ontario, Canada

[2]Institute of Biomedical Engineering, University of Toronto, Toronto, Ontario, Canada

[3]Toronto General Research Institute, University Health Network, Toronto, Ontario, Canada

Abstract

Itaconate (ITA) is an emerging powerhouse of innate immunity with therapeutic potential that is limited in its ability to be administered in a soluble form. We developed a library of polyester materials that incorporate ITA into polymer backbones resulting in materials with inherent immunoregulatory behavior. Harnessing hydrolytic degradation release from polyester backbones, ITA polymers resulted in the mechanism specific immunoregulatory properties on macrophage polarization in vitro. In a functional assay, the polymer-released ITA inhibited bacterial growth on acetate. Translation to an *in vivo* model of biomaterial associated inflammation, intraperitoneal injection of ITA polymers demonstrated a rapid resolution of inflammation in comparison to a control polymer silicone, demonstrating the value of sustained biomimetic presentation of ITA.

One Sentence Summary:

Harnessing the power of innate immunity, we have developed polyester materials that recapitulate the functional effects of itaconate.

1. Introduction

Itaconate (ITA) is a well-known molecule that is evolutionarily preserved in innate immunity [1]. It was first identified during an early investigation of the tricarboxylic acid cycle by Hans Krebs, but was unable to support respiration. This finding lead to a general lack of interest in

*Corresponding author: Institute of Biomedical Engineering, University of Toronto, Toronto, Ontario M5S 3G9, Canada. Tel.: +1-416-946-5295. Fax: +1-416-978-4317. m.radisic@utoronto.ca.

Author contributions: L.D.H. and M.R. conceived the idea, designed the experiments, and analyzed the results. L.D.H. performed the experiments and analyzed the results. L.D.H., Y.W., S.C., B.Y., Y.L., D.B. synthesized and characterized the polymer materials. S.M. assisted in macrophage culture, flow cytometry, and animal models and analysis of these results. Y.W and B.Y. assisted in macrophage culture experiments. S.C., C.E., K.N., and R.M. assisted and advised on in vitro bacterial culture experiments. B.F.L. assisted in mammalian cell culture and analysis of corresponding results. T.B. advised on the polymer synthesis. S.E advised on the in vivo experiments. M.M. assisted in experiments and analyzing the results. L.D.H and M.R. wrote the manuscript. M.R. supervised the entire project. All authors read the manuscript, commented on it, and approved its content.

this biomolecule in the 20th century, with most of its use as a commodity chemical for material development [2].

However, the past 10 years have seen an explosive growth in the new knowledge on this small molecule as an immune regulator, catalyzed by the discovery of ITA production dependent on the immune responsive gene 1 (IRG1)-itaconate axis in macrophages leading to a classical activated inflammatory phenotype after lipopolysaccharide (LPS) stimulation [3]. Initially, it was thought that ITA existed primarily as an antimicrobial metabolite. Under glucose deprived conditions, ITA is a potent inhibitor of isocitrate lyase (ICL) [4], a key enzyme in the microorganism glyoxylate shunt that is often attributed to antibiotic resistivity [5]. Control of bacterial growth has been observed with a number of bacterial strains in the presence of ITA [6], but limitations in efficacy on lipid or acetate carbon sources suggest additional roles of this metabolite in immune regulation.

Importantly, the central role of ITA in metabolic reprograming of macrophage function in inflamed conditions is becoming increasingly clear, where ITA emerged as a powerful anti-inflammatory molecule (Table S1) [7]. Mechanistically, ITA is an enzyme inhibitor of succinate dehydrogenase (SDH) in macrophages [8], and it attenuates inflammation through reduction of succinate oxidation based reactive oxygen species (ROS) generation, a central mechanism of classical inflammatory signaling and activity [9]. The anti-inflammatory characteristics have been demonstrated to be multi-factorial: (a) by effects of ITA on reducing oxidative stress (i.e. ROS and corresponding inflammatory signals) through activation of erythroid 2-related factor 2 (Nrf2) [10]; (b) by ITA regulation of electrophilic stress response along the IκBζ−ATF3 axis that reduced pro-inflammatory factors [10b]; and (c) by ITA reduction of aerobic glycolysis, a key energy pathway in macrophage inflammation, through minimization of GAPDH activity [11]. Consequently, ITA has an impact on osteoclastogenesis [12] and protection from endothelial cell oxidative stress [13]. The molecule represents a potential therapeutic target for the treatment of psoriasis [10b], multiple sclerosis [7], and for immune paralysis in conditions such as sepsis [10].

In the body, ITA is presented by macrophages in a localized on-demand fashion. Unfortunately, oral delivery of ITA results in a rapid removal from circulation within 24 hours, which along with the limited cell membrane permeability, significantly hampers therapeutic potential motivating the development of alternative presentation strategies[10, 14]. Immunomodulatory mechanistic studies have been conducted primarily with highly cell membrane permeable ITA derivatives, including dimethyl itaconate (DMI) [9, 10b] and 4-octyl itaconate[10a, 11, 13], that do not fully overcome the stated limitations. The effective concentration of these derivatives varies according to their electrophilicity[10b], and they are not significantly hydrolyzed intracellularly [15]. These limitations motivate the development of a novel biomimetic presentation strategies.

In practice, local release of bioactive molecules has been achieved through approaches such as physical entrapment and diffusion release from material matrices[16]. In delivery of small molecules similar to ITA, these approaches suffer from limitations such as burst payload release and limited bioactive timelines. Therefore, we looked to a strategy of intelligent polyester chemistry, incorporating ITA into the material backbone structure, to allow for a

biomimetic presentation that enables bioactive anti-inflammatory function (Fig. 1A). We had to overcome undesired non-specific reactivity of the pendant unsaturated group on ITA in generating polymer materials, essential to maintaining immunomodulatory functionality.

In this manuscript, we present the scalable synthesis scheme for incorporation of ITA into a family of polyester material backbones and utilize hydrolytically driven degradation for the quantified sustained presentation of ITA from the material. We demonstrate the ability to recapitulate the regulatory efficacy of ITA in macrophage inflammation, and further demonstrate mechanism specific bacterial growth minimization as a measure of bioactivity. Biomaterial based presentation strategies have wide potential utility, but are often limited by associated inflammation [16–17]. Therefore, we translate the bioactivity of functional ITA polyesters to a model of peritoneal infiltration in response to material implant, wherein we observed improved inflammation resolution in ITA polymer treated groups. Collectively, we provide evidence for the utility of the new polyester platform in bioactive macrophage regulation, opening the possibility for its use as a therapeutic in a number of applications.

2. Results

2.1. Synthesis and processing of ITA containing polyesters

To create a biomaterial that can recapitulate the power of ITA regulation in innate immunity, we used polyester polymer synthesis techniques to incorporate the bioactive molecule into a hydrolytically degradable material. Given the challenge of side reactivity of the pendant acrylate group on ITA, we employed a one-pot polycondensation with methylated carboxylate monomers (DMI) in the presence of a radical inhibitor (4-methoxyphenol, MEHQ) as descried previously [18] (Fig. 1B). Using this method, we have successfully synthesized new polyesters incorporating ITA into the polymer backbone, where we have coupled di-alcohols with ITA to generate long chain polyester materials. By varying the di-alcohol reacted with ITA, we have generated viscous liquid [poly(itaconate-co-hexanediol) (ITA-HD) and poly(itaconate-co-octanediol) (ITA-OD)] and solid [poly(itaconate-co-decanediol) (ITA-DD)] materials (Fig. 1C). Here, we focused on linear polymer materials for simplicity of assessment of material functionality.

After synthesis, the materials present as viscous liquids or solid powders at room temperature (Fig. 1C). In addition to using them as injectable materials, facile processing of the viscous liquids (mixed with Sudan Red for visualization; ITA-HD, Fig. 1D), was demonstrated to generate a surface coating of commonly used medical tubing (ITA-OD, Fig. 1E). Other devices could be similarly coated. Solid formulations can also be processed into scaffolds and coatings using standard techniques. For example, ITA-DD was also solvent cast onto medical grade metal implants at room temperature, presenting stability for storage, transitioning to a viscous liquid when heated to body temperature (37°C) (Fig. 1F).

Chemical structure assessment using proton nuclear magnetic resonance spectroscopy (^{1}H NMR) (Fig. 2A) and Fourier transform infrared spectroscopy (FTIR) (Fig. 2B, Fig. S1) confirmed polymer backbone structure and the presence of the ITA acrylate content, critical for the polymer functionality (peak at 1640 cm^{-1}), when compared to succinate containing materials. Succinate, which lacks the acrylate group, was chosen as a representative control

for synthesis efficacy, given its similarity in backbone structure to ITA (i.e. four carbon carboxylate). Maintenance of this acrylate group is essential for polymer degradability and bioactivity, and the success of our synthesis method was further confirmed by homogenous material appearance and solubility in non-polar solvents including chloroform and ethyl acetate.

2.2. Biomimetic presentation of ITA from new polyesters

Hydrolytic degradation of polyesters was evaluated to determine the release profile of ITA from material backbones. ITA was identified in the m/z spectrum of liquid chromatography-mass spectrometry (LC-MS) assessment of the degradation supernatant of ITA-HD, ITA-OD, and ITA-DD in deionized distilled water (Fig. S2A). Integration of peak area demonstrated an increase in ITA release over 14 days in all materials (Fig. 2C–E). ITA release was notably higher from the solid ITA-DD materials (Fig. 2E) than from the viscous liquid ITA-OD and ITA-HD materials (Fig. 2C–D). This may be attributed to differences in material behavior during purification, where ITA-DD precipitates as a solid in cold methanol, in contrast to ITA-HD and ITA-OD that are viscous liquids. In case of the solid, this process may entrap a greater number of short polymer chains in the material bulk, as it may be harder for the short chains to escape from the solid materials during purification. Upon exposure to a hydrolytic environment, these entrapped shorter chains would be susceptible to a more rapid degradation under culture conditions.

Corresponding diol release was increased over time proportionally to ITA, suggesting degradation release from the polymer backbones (Fig. S2B–D). Gross bulk mass loss was stable under neutral hydrolytic conditions (1x PBS; <2% over 28d) (Fig. 2F), and similarly under slightly alkaline conditions (pH=8) common with *in vivo* environments (Fig. S3). Degradation was accelerated under alkaline conditions (ITA-OD, 1M sodium hydroxide) (Fig. 2G) and in the presence of lipase (ITA-DD) (Fig. 2H), suggesting material susceptibility to hydrolytic and enzymatic degradation and ability to appreciably dissolve over time ITA polyester degradation was comparable to a degradable, commonly used polyester, poly (lactide-co-glycolide) (PLGA) under hydrolytic conditions (Fig. 2F). ITA-OD degraded significantly slower than PLGA in an accelerated alkaline environment (Fig. 2G), minimizing the concerns of localized acidity impacting modulatory properties upon degradation.

The polymers were biocompatible *in vitro* as demonstrated by high viability of human dermal fibroblasts seeded on ITA-OD polymers (live: CFDA-SE, dead: PI; Fig. 2I). Representative images of cells seeded on ITA-OD and stained for viability markers presented no marked difference from tissue culture polystyrene controls.

2.3. ITA polymers recapitulate anti-inflammatory characteristics in vitro

To understand the ITA anti-inflammatory properties of the new polyesters, we differentiated primary murine bone marrow derived macrophages (BMDM) and assessed the impact of polymer treatment on their inflammatory response (Fig. 3A). Given our interest in the degradation release of ITA into the local environment, we coated materials on glass coverslips (18 mm) and used transwell inserts to facilitate ITA release into the culture media

without direct cellular contact (Fig. S4A). Here, we compared inflammatory behavior to similarly degradable PLGA, which we could coat onto glass coverslips in a similar fashion to ITA materials. To benchmark modulation, we also compared to solubilized DMI (0.125 mM), a membrane permeable esterified ITA derivative with previously demonstrated immunomodulatory properties, acting here as a positive control [9–10]. We maintained a high cell viability (Fig. S4B) and monolayer phenotype (Fig. S4C) with treatment and stimulation. There were no appreciable differences in the cell number amongst the treatment groups (Table S2). Cells were treated for 12hr with ITA containing materials, solubilized DMI, PLGA, or media (insert free), then stimulated with LPS (100 ng mL^{-1}, noted as +) or LPS (100 ng mL^{-1}) and IFNγ (50 ng mL^{-1}) (noted as ++) for 12 hr and assessed for cytokine expression and phenotypic response.

Cytokine assessment of pro-inflammatory markers with ELISA demonstrates a significant reduction in inflammation response by cells with ITA containing polyesters (Fig. 3B–N). Due to the same cell number in each group (Table S2), normalization per cell number was not performed for simplicity. Impact on pro-inflammation signaling compared to PLGA and insert free (Blank) controls with similar trend to solubilized DMI (Soluble) was observed following treatment with ITA-DD (Fig. 3B–H), ITA-OD (Fig. 3I–N) and ITA-HD (Fig. S5A–E). Notably, there was a significant reduction in IL-1β (Fig. 3B, I; Fig. S5A), CCL2 (Fig. 3D, K; Fig. S5C), and IL-12p70 (Fig. 3F, M) without noticeable reduction in TNFα expression (Fig. 3E, L; Fig. S5D). Observed reduction in IL-6 (Fig. 3C, J; Fig. S5B) was marked for soluble DMI but limited in polyester treatment. Intriguingly, we were able to replicate the feedback loop identified between ITA, IFNβ, and IRG1 with ITA-DD treatment (Fig. 3H) [10a]. This is reflected in a corresponding regulation of IL-10 through this feedback loop, seen in all ITA polymer treated groups (Fig. 3G, N; Fig. S5E). These outcomes align with the mechanistic behavior of soluble ITA that has been published elsewhere [9–11] (Fig. 3O).

Anti-inflammatory characteristics were prevalent in the nitric oxide phenotypic response of BMDM with ITA containing polymers. Reduction in nitric oxide synthase (NOS2) expression was observed under LPS stimulation with ITA-HD, ITA-OD and ITA-DD treatment, as well as LPS+IFNγ stimulation with ITA-DD treatment, and the expression was similar to soluble DMI treatment (Fig. 4A). A similar trend of downregulation of NOS2 expression with ITA-OD treatment was observed with LPS+IFNγ stimulation when compared to a PLGA control, although slightly less pronounced (Fig. S6). This could be related to a concentration dependency of regulation, given observed differences in ITA molecular release (Fig. 2). Therefore, we focused our NOS2 expression analysis on ITA-DD materials. The differences in NOS2 MFI between ITA-DD treated stimulated groups and controls (PLGA treated and polymer free) were significant under LPS+IFNγ stimulation (Fig. 4C). Although non-significant, there was a similar trend under LPS stimulation conditions (Fig. 4B). NOS2 is expressed in a lower quantity under LPS stimulation alone, and therefore we do not expect to see a significant difference in MFI between the groups under such conditions. Importantly, in both cases (LPS and LPS+IFNγ stimulation) significant differences are observed in nitrite reduction (which is a product of NOS2) following treatment with viscous liquid (ITA-HD, ITA-OD) (Fig. 4D) and solid (ITA-DD) (Fig. 4E) polyester material, further supporting trends in NOS2 expression. Coupled with

cytokine assessment, these outcomes suggest that the anti-inflammatory behavior of the degradation released ITA from the polymer materials can recapitulate the inflammatory behavior of ITA *in vitro.*

2.4. Mechanism specific antibacterial properties demonstrate bioactivity of polymer released ITA

Given the observed modulation of inflammatory behavior, we used the known bacterial growth modulation of ITA through glyoxylate shunt inhibition as an assay of ITA polymer specific bioactivity. Given that ITA is a potent inhibitor of ICL, important for persistent bacterial growth on 2-carbon substrates (i.e. acetate) through the glyoxylate shunt [4] (Fig. 5A), we benchmarked *in vitro* material efficacy on bacterial growth modulation in minimal media (M9) with an acetate carbon source (1% m/v). Given known inhibitory characteristics of acetate at moderate concentrations, we optimized the acetate concentration in M9 media until conditions suitable for nearly maximal *E. coli* growth were identified (Fig. S7A). We used *E. coli* as a model organism given well understood growth behavior under these conditions.

Culture of *E. coli* with soluble ITA (neutralized acid) under these conditions yielded growth reduction at concentrations of soluble ITA as low as 1mM (measured by OD: 600nm) (Fig. S7B). This inhibition was not observed with a glucose carbon source (0.4% m/v) (Fig. S7C), or on rich media (LB broth) (Fig. S7D), consistent with previously observed inhibition specificity [19]. Culture with soluble DMI, presented similar effects on bacterial growth in acetate conditions (Fig. S7E) with addition of some sensitivity (>7.5 mM) on rich media (Fig. S7F).

Growth inhibition from polymer degradation was assessed by measuring optical density of bacteria in well plates. Here, ITA-HD, ITA-OD and ITA-DD demonstrated a profound bacterial growth reduction compared to the polymer-free controls under acetate growth conditions (Fig. 5B). Remarkably, when compared to commercially available silver nanoparticles, a current gold standard in antimicrobial materials, ITA-DD exhibited similar bacterial growth inhibition (no significant difference between silver and polymer groups) (Fig. 5C). Silver doping has been used widely in biomaterials, but has met some limited efficacy due to observed systemic toxicity[20]. Importantly, the regulatory behavior of ITA polymers was specific to growth conditions. Culture of ITA-OD and ITA-DD in the media conditions with a glucose carbon source did not present any appreciable inhibition (Fig. 5D), and only slight inhibition for ITA-DD on LB broth (Fig. 5E) suggesting the specificity of inhibition to acetate conditions (Fig. 5B). Given the known specificity of ITA growth inhibition to conditions that require the glyoxylate shunt[4] (e.g. acetate conditions), the lack of impact on growth on defined media with glucose and LB broth suggested the ITA polyesters recapitulate soluble ITA efficacy. Both glucose containing M9 media and LB broth contain nutrients that enable the bacterial cells to create the needed energy through the tri-carboxylic acid (TCA) cycle (i.e. glucose metabolism), which is not affected by the presence of ITA. However, under limited nutrient growth conditions, bacteria activate the glyoxylate shunt, a shorter anabolic pathway that employs ICL to convert isocitrate to

glyoxylate, ultimately shortcutting the TCA to generate malate. ITA is known to inhibit ICL, thus effectively inhibiting bacterial metabolism under nutrient limited conditions.

To validate that ITA polymer efficacy was not an artifact of non-specific material behavior, we did comparative analyses with other degradable polyester materials. Of these controls, PLGA is known to create acidic environment during degradation [21], thus it was an appropriate control for non-specific acidity effects on bacterial growth. When compared to widely used biomaterials, degradable PLGA and viscous liquid silicone, the control materials did not exhibit bacterial growth reduction, whereas ITA-OD and ITA-DD maintained significant reduction in growth comparable to solubilized ITA (1mM) (Fig. 5F). This further suggests the mechanistic specificity of degradable ITA polyesters, as degradable PLGA with acidic byproducts did not provide inhibitory behavior. This outcome was also reflected when comparing to poly(adipate–co-octanediol) (ADI-OD), which was synthesized under the same polymerization approach (Fig. 5G), suggesting the ITA content in polymers was responsible for inhibition. Polymer based growth reduction was reproducible across three independent synthesis batches of ITA-HD (Fig. 5H). With ITA-DD materials, the inhibition was tunable according to polymer reaction times, suggesting the potential for material optimization for the desired application (Fig. 5I).

2.5. Resolution of biomaterial associated inflammation

Given the mechanistic efficacy of ITA with a biomimetic presentation from a polymer, we looked to translate this immunomodulation to a model of biomaterial associated inflammation. Herein, we used a viscous liquid silicone (viscosity:13.99 ± 0.15 Pa.s) in a peritoneal model of immune cell infiltration as a control of similar appearance and consistency to ITA-OD (viscosity: 42.59 ± 0.43 Pa.s) (Fig. S8). Silicone was selected as a synthetic, injectable, viscous liquid control [17] that is also known to develop a typical frustrated biomaterial immune response [22]. Importantly, we focused on selection of a material with comparable material properties (i.e. injectable, viscous liquid) to assess differences in cell response based on material composition. Material (ITA-OD, viscous liquid silicone) or a saline injection into murine peritoneal cavity was employed to assess immune cell recruitment (Fig. 6A).

Due to the known complexity of the host response, we used single cell extraction and assessment with multi-color flow cytometry (Fig. S9) to identify and quantify populations of neutrophils ($Ly6G^+$, $Ly6C^+$), early monocytes ($Ly6C^+$), eosinophils ($CD193^+$), and resident macrophages ($CD102^+$, $F4/80^+$) (Fig. 6). Acute response (day 3) to ITA-OD and silicone demonstrated a comparable acute loss of the resident macrophage population, and comparable acute increase across cell types and material groups (Fig. 6C–F). Representative flow cytometry plots of ten days post-injection present decreased neutrophil and $Ly6c^{Hi}$ monocytes in ITA-OD groups as a percentage of total live cell population in comparison to silicone controls (Fig. 6B). Comparison of absolute inflammatory cell numbers further highlighted this difference; cell number remained consistent in silicone groups (day 3 and day 10), suggesting prolonged frustrated inflammation, whereas inflammation resolved with ITA polymers in the three assessed inflammatory cell populations (Fig. 6C–F). Although the percentage of eosinophils in the representative flow plots is similar in the ITA-OD and

Silicone treated groups (Fig. 6B), the total number of live cells infiltrating is lower in the ITA-OD compared to the Silicone groups (Fig. 6F). Two-way ANOVA rigorously demonstrated the significance of treatment (ITA-OD vs. Silicone vs. Saline) on resolution of inflammatory cell infiltration (Fig. 6). Therefore, quantitative outcomes suggest that the initial acute response to material implantation is maintained, but our biomimetic polyesters play a modulating role on biomaterial associated frustrated inflammation. Overall, these findings demonstrate translation of ITA immunomodulatory effects beyond macrophage behavior.

3. Discussion

ITA has recently emerged as a powerful regulator in innate immunity, presenting opportunity in developing anti-inflammatory therapeutics that harness this efficacy. It is difficult to deliver it using traditional oral systemic strategies, given its small molecule carboxylic acid structure. This is also true for its other small molecule derivatives (e.g. DMI). In fact, orally delivered ITA of up to 2 grams in rats was rapidly removed in 24 hours [14]. Therefore, we have proposed and demonstrated here the development of hydrolytically degradable ITA polymers that accomplish this goal.

The development of degradable polymer constructs that incorporate ITA in its original structure, i.e. maintenance of its pendant unsaturated carbonyl, is nontrivial. Due to the high reactivity of the pendant unsaturated carbonyl, initial trials presented challenges with side reactions. Here, we have demonstrated the reproducible maintenance of the molecular structure, ensuring potential for molecular release in desired applications. The bulk mass stability of ITA containing materials over one month in deionized water is comparable to widely studied polyester materials, including PLGA [23], and poly(glycerol sebacate) [24], which suggests the long term active potential of ITA material-based constructs as these materials slowly degrade over months to years under such conditions.

Biomimetic presentation of ITA through polymers could amplify observed cellular activity. Beyond the known effects of ITA, novel biomaterial properties include: (1) multiple reactive sites: hydroxyl, carboxylate, and pendant unsaturated carbon-carbon for on-demand post-reactivity; (2) melting at approximately physiological conditions which imparts on-shelf stability, followed by a transition to liquid form compatible with soft tissue application *in vivo;* and (3) one pot synthesis of a pure product via a facile and green-friendly chemistry. Opportunity to further optimize these properties exists given the breadth of di-alcohols and co-polymerization candidates that can be leveraged in polyester based synthesis techniques.

Use of multiple material controls allowed us to understand the multimodal efficacy of ITA-containing materials in biological microenvironments. Comparison to PLGA *in vitro* enabled benchmarking against well understood degradable materials, with minimized interaction of cells with material surfaces to limit impact of material property differences. In an *in vivo* setting, we matched mechanical material properties as much as possible, to enable the comparison of polymer composition on cell infiltration which motivated our selection of silicone in contrast to ITA-OD. In addition, we chose to apply the material by injection rather than surgically, as background immune response is significantly higher with surgical

intervention. We leveraged an injection into this cavity to minimize the background response (as demonstrated by the saline only group). PLGA was therefore not an appropriate control in this experiment since it is a solid material and require surgical implantation. Comparison of new polyesters to silicone gave contrast to a material known to elicit a typical frustrated biomaterial associated immune response.

Mechanistically, degradation products from ITA polymers recapitulate behavior of the multiple proposed immunoregulatory mechanisms. Here, we focused on functional assessment of cytokine secretion under inflammatory treatment as a measure of regulation. Previous studies have described two primary anti-inflammatory functions of ITA; (1) a competitive SDH enzyme inhibitor, which presented a downregulation in ROS based inflammation [9–10], and (2) as a modifier of protein regulators (2,3-dicarboxylpropylation) including Nrf2 [10a], glutathione [10b], GADPH [11], and ATF3 [10b] to modify inflammation. Transwell culture with ITA polymers demonstrated downregulation of IL-1β, IL-12p70, and IL-6 in a similar manner as soluble DMI. The magnitude of regulation varied according to cytokine and material, which may indicate differences in concentration thresholds as has been described previously [9–10, 11].

Here, we also present the ITA-based regulation of CCL2, which has demonstrated links to Nrf2 and IκBζ axes and was strongly observed in polymer treated groups [25]. Intriguingly, we detected a strong relationship in the previously identified feedback loop between IFNβ and ITA-DD treatment, that is seen through a strong downregulation in IL-10 in all material treated groups [10a]. IL-10 can play multiple signaling roles, and under induced inflammatory conditions tends to be upregulated [26]. In this study, the effective reduction of IFNβ related response by ITA regulation is tied to a reduction in IL-10 secretion. The feedback loop between IL-10 and IFNβ captured here may open interesting therapeutic avenues. Further, IL-10 does primarily serve as a regulator of excessive inflammation under LPS activation [26]; thus the reduced expression of this cytokine under such conditions is an indicator of a holistic decrease in macrophage inflammation with ITA treatment.

Perhaps most critically, TNFα is consistently unaffected, reflecting this consistency across prior mechanistic studies [7]. Phenotypically, we present the downregulation of NOS2 expression and corresponding nitrite secretion. This further supports the ability of ITA polymers to regulate ROS driven inflammation in inflammatory macrophages. In future study in the context of biomaterials, consideration of modulation under other stimulation conditions (i.e. IL-4/IL-10) *in vitro* may further expand the novelty of this ITA modulation approach.

Although mechanistic regulatory properties of ITA are known, the molecule is only generated by macrophages under inflammatory stress (i.e. infection, LPS). Our polymer allows for the continuous presence of the molecule over time to accomplish therapeutic goals under all conditions. Membrane diffusion has been demonstrated across the mitochondrial membrane through the active transport carrier, dicarboyxlate, and may suggest existence of other pathways for ITA passage into the cytosol [10a]. Suggested potential of an unidentified ITA extracellular membrane receptor further lends to the application of ITA at the material surface [15]. Exploration of the role of ITA in activated

macrophages and other immune cells is still in its infancy, presenting potential opportunity for regulatory ITA-based biomaterials to aid in further mechanistic studies [27].

We further confirmed the ability for ITA polymers to perform ITA functions through known modulation of bacterial growth on the glyoxylate shunt. These outcomes presented strong reduction of *E. coli* growth in suspension culture in all of our material groups, supporting the outcomes we present in functional immunomodulation. Importantly, the stark specificity of activity to acetate growth substrates, and the inability of similar materials, made without ITA, to impact *E. coli* growth, highlights the bioactivity of ITA released through polyester degradation. Interestingly, the role of ITA in pathogenic prevention may not be completely understood, given that multiple strains have identified degradation pathways for the molecule [28] and its value in synergistic immune cell restriction of persistent growth [7]. Importantly, ICL has been shown to be important in persistent virulence, which may indicate a greater value of ITA based materials in application with virulent pathogens [29].

We present here the power of bioactivity in polymer design in the context of biomaterial associated inflammation. The use of polymer-based biomaterial implants in healthcare has been extensively reported[16, 30], but many of these devices are subject to limited efficacy due to poor interaction with host immunity[31]. Traditionally, design approaches have focused on achieving inert behavior, masking implants from the cellular system of the host with a focus on achieving mechanical function while remaining biologically inert[32]. Although this approach has allowed for a number of clinical successes, there is an opportunity to leverage mechanistic cues from host immunity to better utilize biomaterials[33]. We achieved this here by incorporating ITA directly into polymers to impart bioactivity. The ultimate result was a significant reduction in the quantity and type of infiltrated myeloid cells ten days post implantation when compared to a silicone control, which is known to exhibit a typical foreign body response [34]. This presents value of ITA polyester application to efficiently limit the duration and nature of the inflammatory response. Leveraging this, in the future, ITA-based biomaterials may provide a platform for potential uses in compartmentalized chronic auto-immune conditions, such as rheumatoid arthritis, where sustained local release within the joint space has potential to improve treatment-resistant disease [35].

In summary, a family of degradable polymer materials containing ITA was developed to improve the therapeutic potential of this powerful regulator of innate immunity. Uniquely, this approach allowed for sustained delivery of a multifunctional bioactive molecule, and consistently recapitulated the known specificity of ITA mechanistic regulation. In building a bioactive material, we demonstrate resolution of associated inflammation, an important feature for effective material adoption, and suggest the value of the multi-modal impact of this biomaterial based delivery platform. These biomaterials fulfill multiple roles in a similar manner that cells do, translating the regulatory behavior of ITA to a scalable delivery platform. As the new roles and mechanisms of ITA continue to emerge, sustained delivery strategies through intelligent polymers will become instrumental in leveraging therapeutic impact.

4. Materials and Methods

4.1. Materials

ITA (99%), DMI (99%), 1,6-hexanediol (HD, 97%), 1,8-octanediol (OD, 98%), 1,10-decanediol (DD, 98%), tin (II) ethylhexanoate (92.5–100%), MEHQ (99%), chloroform-d ($CDCl_3$, 99.8%), PLGA (lactide:glycolide (75:25), M_w: 66,000 – 107,000), diethyl succinate (99%), diethyl adipate (99%), ammonium acetate (99%), 3-(N-morpholino)propanesulfonic acid) (MOPS, 1M), LB (Lennox) broth, silver nanoparticles (particle size: 10nm), EDTA, lipase from Thermomyces lanuginosus, and LPS (from *E. coli* O111:B4) were purchased from Sigma Aldrich (St. Louis, MO). Sodium acetate (99%), glucose (99.5%), salts used in M9 minimal media (Na_2HPO_4, KH_2PO_4, NaCl, NH_4Cl, $MgSO_4$, $CaCl_2$; >99%), thiamine (99%), methanol (99.8%) (MeOH) and sodium hydroxide (10N) (NaOH) were purchased from BioShop Canada (Burlington, ON). Ethanol (anhydrous) was purchased from Commercial Alcohols (Brampton, ON). Dulbecco's modified Eagle's medium, RPMI 1640 with L-glutamine, fetal bovine serum (FBS), penicillin-streptomycin, N-2-hydroxyethylpiperazine-N-2-ethane sulfonic acid (HEPES), GlutaMax supplement, Dulbecco's phosphate buffered saline (DPBS), (5-(and-6)-Carboxyfluorescein Diacetate, Succinimidyl Ester) (CFDA-SE), propidium iodide (PI), 4′,6-diamidino-2-phenylindole (DAPI) UltraComp eBeads, ArC Amine Reactive Compensation Bead Kit, ACK lysis buffer and paraformaldehyde were purchased from ThermoFisher Scientific (Waltham, MA). Mouse recombinant macrophage colony stimulating factor (MCSF) and mouse recombinant interferon gamma (IFNγ) were purchased from Miltenyi Biotec (Bergisch Gladbach, Germany). Griess reagent kit was purchased from Cell Signaling Technology (Danvers, MA). Antibody stains used in flow cytometry were purchased from Biolegend (San Diego, CA) unless otherwise noted. All materials were used as received unless otherwise described.

4.2. Polymer synthesis

Polyester materials containing ITA were prepared using DMI in combination with long chain di-alcohols (i.e. 1,6-hexanediol, 1,8-octanediol, 1,10-decanediol). Monomers were added to a 250 mL triple-neck flask in equimolar amounts with MEHQ (0.5 wt%) as an inhibitor of radical polymerization and tin (II) ethylhexanoate (2 mol%) as a catalyst. The mixture was heated to 130°C to generate a bulk melt polymerization solution. The reaction solution was stirred at 200 rpm for 6 hr under nitrogen purge followed by a slow reduction of pressure to vacuum and a further 12 hr of reaction, or for times as indicated. Polymers were purified through precipitation in cold MeOH (−80°C) followed by solution decanting and drying of the polymer material. Materials containing other dicarboxylic acids (dimethyl succinate, diethyl adipate) were prepared as described with substitution of DMI with the appropriate carboxylate monomer.

4.3. Polymer Characterization

Polymer structure was confirmed using ^1H NMR on an Agilent DD2 600 MHz spectrometer. Polymer samples were dissolved in $CDCl_3$. Chemical shifts were tested against the resonance of protons in internal tetramethylsilane. Peak assessment and integration was conducted using MNova software to validate material structure and determine limitation of undesired radical polymerization. Samples were also characterized by ATR-FTIR (Perkin

Elmer Spectrum One). Assessment included 32 scans as percent transmittance from 4000 to 550 cm^{-1} at a resolution of 4 cm^{-1} and corrections for ATR, baseline and smoothing. Viscosity measurements were performed using a TA Instruments Discovery HR-2 hybrid rheometer. A flow sweep was performed at sheer rates from 0.1 1/1 1/s (7 points, 20°C)

4.4. Bulk Degradation

To assess mass loss, materials (100 mg) were cast on the base of glass vials (20 mL) of known mass and incubated with 2.5 mL of deionized distilled water for indicated time points. At endpoint, supernatant was collected for mass spectroscopy assessment, then dried (48 hr, 75°C) and weighted for final mass. Accelerated degradation was assessed under alkaline conditions (EDTA (500 mM), pH 8.0, or 1M NaOH) and in a solution containing lipase (5000 U g^{-1} polymer) for indicated times using the same method. The degree of degradation was calculated by comparing the dry mass of the polymer film after degradation and the initial mass.

4.5. Mass spectroscopy assessment

LC-MS analysis was performed using a Dionex Ultimate 3000 UHPLC system and a Q-Exactive mass spectrometer equipped with a HESI source (all from Thermo Scientific) and controlled by Thermo XCalibur 4.1 software. LC separation was conducted on a Hypersil Gold C18 column (50 mm × 2.1 mm, 1.9 μ particle size, Thermo Scientific) equipped with a guard column. Solvent A was 5mM ammonium acetate in water (pH 6), and solvent B was 5mM ammonium acetate in MeOH (pH 6). The column was run at a flow rate of 300A μL min^{-1} and at a column temperature of 40°C. Autosampler temperature was maintained at 8 °C, and injection volume was 10 μL. The gradient was 0–1 min: 2% B; 1–7 min: linear gradient to 98% B; 7–10 min: 98% B; 10–10.5 min: linear gradient to 2% B; 10.5–15 min: 2% B. Data collection was done in positive and negative ionization modes with a scan range m/z 100–1000, resolution 140 000 at 1 Hz, AGC target of 3e6 and a maximum injection time of 200 ms. Standard solutions of ITA ([M-H]- = 129.0193), HD ([M+H]+ = 119.1067), OD ([M+H]+ = 147.1380), and DD ([M+H]+ = 175.1693) were used for validation of retention time and m/z. Molecular release was interpreted as area under respective m/z peaks.

4.6. Screening fibroblast cell attachment and viability on polymer sheets

To assess cell attachment and viability, ITA-OD was cast in 24-well plates (0.2 mL) to form a thin polymer sheet. Prior to cell seeding, wells were thoroughly rinsed with PBS and sterilized with 70% ethanol (30 min) followed by three washes in PBS. Dermal fibroblasts were seeded in coated wells or uncoated controls (tissue culture polystyrene) at 1.8×10^4 cells cm^{-2}, cultured in DMEM supplemented with 10% fetal bovine serum, Glutamax (1%) and Pen/Strep (100 U mL^{-1}). Two days post-seeding, cell viability was assessed using CFDA-SE (1:1000) and PI (1:200) in DPBS (30 min, 37°C) followed by fixation in 4% paraformaldehyde (30 min). Cells were counter-stained with DAPI (1:1000) and imaged with an Olympus fluorescent microscope. Adhered viable cells were counted using the IMARIS 8 image analysis and compared between experimental groups.

4.7. Material coating

To demonstrate material application, ITA-HD and ITA-OD was combined with Sudan IV in ethyl acetate (0.8 mg mL^{-1}) and coated on the inner wall of silicone tubing with slow rotation during solvent evaporation. Coating of ITA-DD on metal alloy was done by dropwise solvent casting (0.8 mg mL^{-1}) dissolved in ethyl acetate.

4.8. Bone marrow-derived macrophage culture

Macrophage cells were isolated from 6–12 week old C57BL/6 mice as described previously[36] and cultured in RPMI-1640 medium with L-glutamine supplemented with 10% heat inactivated FBS, penicillin-streptomycin (100 U mL^{-1}) and MCSF (20 ng mL^{-1}) for seven days. For experiments, cells were seeded at 90,000 cells cm^{-2} in 6 well culture plates, in RPMI-1640 medium with L-glutamine supplemented with 10% heat inactivated FBS and penicillin-streptomycin (100 U mL^{-1}). Cells were treated with ITA-DD, ITA-OD, ITA-HD, or PLGA (200mg coated on glass coverslips; diameter = 18 mm) in transwell inserts (8 μm pore size), soluble DMI (0.125 mM), or media only for 12 hr, then activated with LPS (100 ng mL^{-1}), or LPS (100 ng mL^{-1}) and IFNγ (50 ng mL^{-1}) for 12 hr prior to assessment. Unstimulated cells treated with identical groups were used as a negative control.

4.9. Quantification of cytokines and nitric oxide

Cytokine quantification was conducted on cell supernatants using a mouse 10-plex pro-inflammatory assay or an interferon beta single plex assay (Eve Technologies, Calgary, AB) and calculated using the provided standard curves. Nitrite content was determined using a Griess Reagent Kit.

4.10. *In vitro* E. coli bacterial growth assessment

E. coli (BL21) was expanded overnight in LB broth, then seeded (1:100) in fresh medium according to growth conditions. Experiments with different treatment groups were carried out either in: modified M9 minimal salts medium[37] (6.78 g L^{-1} Na_2HPO_4, 3.0 g L^{-1} KH_2PO_4, 0.5 g L^{-1} NaCl, 1.0 g L^{-1} NH_4Cl, 1 mM $MgSO_4$, 0.1 mM $CaCl_2$) supplemented with thiamine (0.5 g L^{-1}), MOPS (100mM), a mixture of trace metals described elsewhere[38], and an appropriate carbon source (Acetate: 1%, Glucose 0.4%, m/v); or LB broth (Lennox) for rich media experiments. Acetate concentration (1–3% (m/v)) was optimized in M9 media prior to execution of these experiments. Time course assessment of soluble small molecule inhibition was conducted in 96-well culture plates fitted with a breathable film to encourage aeration and cultured for indicated time with incremental optical density measurement (600 nm). Growth media containing solubilized acid was neutralized with sodium hydroxide (pH = 7.0).

To determine polymer antimicrobial properties in solution, six well plates were cast with equal mass polymer samples and polymer free culture plate (polystyrene) controls. Plates were sealed with a plastic film to prevent media evaporation (3 mL/well) and cultured for four days (37°C, 100 rpm) in media conditions indicated in the text (i.e. M9 with defined carbon source or LB broth), with daily growth assessment by extraction of media (100 μL) to measure change in optical density (600 nm). Silver nanoparticles (10 nm) and soluble neutralized ITA were used as positive controls. PLGA and viscous liquid silicone were used

as negative controls. Soluble assessment of DMI was conducted using the method described for polymer samples using a 12 well plate format (1.5 mL/well).

4.11. Animal study ethics

Experiments in this work involving animals were conducted under the *Guide to the Care and Use of Experimental Animals* from the Canadian Council on Animal Care and Procedures approved by the Animal Care Committees of the University of Toronto and University Health Network (Toronto, Canada).

4.12. Peritoneal Material Implantation Study

An immune cell infiltration model in the peritoneal cavity was used to assess host response to implanted materials. Injected materials were prepared by sterilizing in 70% ethanol and washed in DPBS followed by drying under sterile vacuum conditions (3 days). Adult C57BL/6 mice (6–8 weeks old, Charles River Laboratories, USA) were injected (50 μL) with ITA-OD, silicone, or saline (Sham) using a 18G needle into the peritoneal cavity. Three or ten days post implantation, animals were euthanized and the peritoneal cavity was washed with DPBS (10 mL) to extract single cell infiltrates. Cells were concentrated, treated with ACK lysis buffer to remove red blood cells (1 mL, 5 min), washed with DPBS, then counted and assessed by flow cytometry.

4.13. Flow Cytometry

Cells analyzed by flow cytometry were concentrated (2 million/100 μL), washed with DPBS and stained with Zombie Violet Fixable Viability Kit (1:500; RT, 20 min), blocked with anti-CD16/32 (RT, 10 min), and surface stained according to experimental protocol (4°C, 30 min). *In vitro* studies with BMDMs were stained with anti-F4/80 and anti-CD11b, fixed in 4% paraformaldehyde, permeated (Permeabilization Buffer, eBioscience), and stained for anti-NOS2 (Santa Cruz Biotechnology) (Antibody Clones: Table S3). Cells were gated for viability and $F480^{+}/CD11b^{+}$ cells prior to assessment of median fluorescence intensity (MFI) for NOS2 expression. Peritoneal single cell extracts were surface stained with a multi-colour immune cell panel (Gating: Fig. S9, Antibody Clones: Table S3). Compensation and positive staining were performed for each experimental run with UltraComp eBeads and ArC Amine Reactive Compensation Bead Kit. Flow cytometric assessment was conducted on a BD LSRII-OICR Cytometer (Flow and Mass Cytometry Facility, University Health Network, Toronto, ON). Data acquisition was done with BD FACS Diva software, analyzed with FlowJo (BD) software. Immune cell number in peritoneal extracts was determine as relative abundance against a manual cell count conducted prior to staining.

4.14. Statistical Analysis

All bar graph data are presented as the mean ± standard deviation (s.d.) unless otherwise indicated. Sample sizes (n) indicate biological replicates or number of animals. Normality and equality of variance were tested before a statistical test. Significance was measured as indicated for each experiment, either with a student t-test, or with one way or two way ANOVA followed by pairwise comparison with Tukey's multiple comparisons test using Graphpad Prism 8; *$p<0.05$, **$p<0.01$, ***$p<0.001$, ****$p<0.0001$

Supplementary Material

Refer to Web version on PubMed Central for supplementary material.

Acknowledgements

The collection, analysis, and expertise in mass spectroscopy assessment provided by Robert Flick of the BioZone Mass Spectrometry Facility, University of Toronto is highly acknowledged.

Funding:

This work was funded by the Heart and Stroke Foundation Grant-in-Aid (G-16-00012711), Natural Sciences and Engineering Research Council of Canada (NSERC) Discovery Grant (RGPIN 326982-10), NSERC-CIHR Collaborative Health Research Grant (CHRP 493737-16) and National Institutes of Health Grant 2R01 HL076485. MR was supported by NSERC Steacie Fellowship and Canada Research Chair, LDH was supported by CIHR Vanier Scholarship. The authors acknowledge the Canada Foundation for Innovation, Project 19119, and the Ontario Research Fund for funding of the Centre for Spectroscopic Investigation of Complex Organic Molecules and Polymers.

References

[1]. Luan HH, Medzhitov R, Cell Metab 2016, 24, 379. [PubMed: 27626199]

[2]. Cordes T, Michelucci A, Hiller K, Annual review of nutrition 2015, 35, 451.

[3]. a)Strelko CL, Lu W, Dufort FJ, Seyfried TN, Chiles TC, Rabinowitz JD, Roberts MF, Journal of the American Chemical Society 2011, 133, 16386; [PubMed: 21919507] b)Shin JH, Yang JY, Jeon BY, Yoon YJ, Cho SN, Kang YH, Ryu DH, Hwang GS, J Proteome Res 2011, 10, 2238; [PubMed: 21452902] c)Sugimoto M, Sakagami H, Yokote Y, Onuma H, Kaneko M, Mori M, Sakaguchi Y, Soga T, Tomita M, Metabolomics 2011, 8, 624.

[4]. a)McFadden B, Purohit S, Journal of bacteriology 1977, 131, 136; [PubMed: 17593] b)Rittenhouse JW, McFadden BA, Archives of biochemistry and biophysics 1974, 163, 79. [PubMed: 4852477]

[5]. Garaude J, Acin-Perez R, Martinez-Cano S, Enamorado M, Ugolini M, Nistal-Villan E, Hervas-Stubbs S, Pelegrin P, Sander LE, Enriquez JA, Sancho D, Nat Immunol 2016, 17, 1037. [PubMed: 27348412]

[6]. a)Michelucci A, Cordes T, Ghelfi J, Pailot A, Reiling N, Goldmann O, Binz T, Wegner A, Tallam A, Rausell A, Buttini M, Linster CL, Medina E, Balling R, Hiller K, Proceedings of the National Academy of Sciences 2013, 110, 7820;b)Naujoks J, Tabeling C, Dill BD, Hoffmann C, Brown AS, Kunze M, Kempa S, Peter A, Mollenkopf HJ, Dorhoi A, Kershaw O, Gruber AD, Sander LE, Witzenrath M, Herold S, Nerlich A, Hocke AC, van Driel I, Suttorp N, Bedoui S, Hilbi H, Trost M, Opitz B, PLoS Pathog 2016, 12, e1005408. [PubMed: 26829557]

[7]. O'Neill LAJ, Artyomov MN, Nat Rev Immunol 2019, DOI: 10.1038/s41577-019-0128-5.

[8]. Cordes T, Wallace M, Michelucci A, Divakaruni AS, Sapcariu SC, Sousa C, Koseki H, Cabrales P, Murphy AN, Hiller K, Metallo CM, The Journal of biological chemistry 2016, 291, 14274. [PubMed: 27189937]

[9]. Lampropoulou V, Sergushichev A, Bambouskova M, Nair S, Vincent EE, Loginicheva E, Cervantes-Barragan L, Ma X, Huang SC, Griss T, Weinheimer CJ, Khader S, Randolph GJ, Pearce EJ, Jones RG, Diwan A, Diamond MS, Artyomov MN, Cell Metab 2016, 24, 158. [PubMed: 27374498]

[10]. a)Mills EL, Ryan DG, Prag HA, Dikovskaya D, Menon D, Zaslona Z, Jedrychowski MP, Costa ASH, Higgins M, Hams E, Szpyt J, Runtsch MC, King MS, McGouran JF, Fischer R, Kessler BM, McGettrick AF, Hughes MM, Carroll RG, Booty LM, Knatko EV, Meakin PJ, Ashford MLJ, Modis LK, Brunori G, Sevin DC, Fallon PG, Caldwell ST, Kunji ERS, Chouchani ET, Frezza C, Dinkova-Kostova AT, Hartley RC, Murphy MP, O'Neill LA, Nature 2018, DOI: 10.1038/nature25986;b)Bambouskova M, Gorvel L, Lampropoulou V, Sergushichev A, Loginicheva E, Johnson K, Korenfeld D, Mathyer ME, Kim H, Huang LH, Duncan D, Bregman H, Keskin A, Santeford A, Apte RS, Sehgal R, Johnson B, Amarasinghe GK, Soares MP, Satoh

T, Akira S, Hai T, de Guzman Strong C, Auclair K, Roddy TP, Biller SA, Jovanovic M, Klechevsky E, Stewart KM, Randolph GJ, Artyomov MN, Nature 2018, DOI: 10.1038/s41586-018-0052-z.

[11]. Liao ST, Han C, Xu DQ, Fu XW, Wang JS, Kong LY, Nature communications 2019, 10, 5091.

[12]. Sun X, Zhang B, Pan X, Huang H, Xie Z, Ma Y, Hu B, Wang J, Chen Z, Shi P, FASEB J 2019, DOI: 10.1096/fj.201900887RRfj201900887RR.

[13]. Tang C, Tan S, Zhang Y, Dong L, Xu Y, Biochem Biophys Res Commun 2018, DOI: 10.1016/j.bbrc.2018.12.032.

[14]. Booth AN, Taylor J, Wilson RH, DeEds F, Journal of Biological Chemistry 1952, 195, 697.

[15]. ElAzzouny M, Tom CT, Evans CR, Olson LL, Tanga MJ, Gallagher KA, Martin BR, Burant CF, The Journal of biological chemistry 2017, DOI: 10.1074/jbc.C117.775270.

[16]. Davenport Huyer L, Pascual-Gil S, Wang Y, Mandla S, Yee B, Radisic M, Advanced Functional Materials 2020, 1909331.

[17]. Sadtler K, Wolf MT, Ganguly S, Moad CA, Chung L, Majumdar S, Housseau F, Pardoll DM, Elisseeff JH, Biomaterials 2019, 192, 405. [PubMed: 30500722]

[18]. a)Winkler M, Lacerda TM, Mack F, Meier MAR, Macromolecules 2015, 48, 1398;b)Davenport Huyer L, Bannerman AD, Wang Y, Savoji H, Knee-Walden EJ, Brissenden A, Yee B, Shoaib M, Bobicki E, Amsden BG, Radisic M, Advanced healthcare materials 2019, DOI: 10.1002/adhm.201900245e1900245.

[19]. Hammerer F, Chang JH, Duncan D, Ruiz AC, Auclair K, Chembiochem 2016, DOI: 10.1002/cbic.201600078.

[20]. Park MV, Neigh AM, Vermeulen JP, de la Fonteyne LJ, Verharen HW, Briede JJ, van Loveren H, de Jong WH, Biomaterials 2011, 32, 9810. [PubMed: 21944826]

[21]. Fu K, Pack DW, Klibanov AM, Langer R, Pharmaceutical research 2000, 17, 100. [PubMed: 10714616]

[22]. a)Dalu A, Blaydes BS, Lomax LG, Delclos KB, Biomaterials 2000, 21, 1947; [PubMed: 10941916] b)James SJ, Pogribna M, Miller BJ, Bolon B, Muskhelishvili L, Biomaterials 1997, 18, 667; [PubMed: 9151998] c)Farah S, Doloff JC, Muller P, Sadraei A, Han HJ, Olafson K, Vyas K, Tam HH, Hollister-Lock J, Kowalski PS, Griffin M, Meng A, McAvoy M, Graham AC, McGarrigle J, Oberholzer J, Weir GC, Greiner DL, Langer R, Anderson DG, Nature materials 2019, 18, 892. [PubMed: 31235902]

[23]. a)Yang S, Leong K-F, Du Z, Chua C-K, Tissue engineering 2001, 7, 679; [PubMed: 11749726] b)Engelberg I, Kohn J, Biomaterials 1991, 12, 292. [PubMed: 1649646]

[24]. Pomerantseva I, Krebs N, Hart A, Neville CM, Huang AY, Sundback CA, Journal of biomedical materials research. Part A 2009, 91, 1038. [PubMed: 19107788]

[25]. a)Eitas TK, Stepp WH, Sjeklocha L, Long CV, Riley C, Callahan J, Sanchez Y, Gough P, Knowlin L, van Duin D, Ortiz-Pujols S, Jones SW, Maile R, Hong Z, Berger S, Cairns BA, PLoS One 2017, 12, e0184164; [PubMed: 28886135] b)Hildebrand DG, Alexander E, Horber S, Lehle S, Obermayer K, Munck NA, Rothfuss O, Frick JS, Morimatsu M, Schmitz I, Roth J, Ehrchen JM, Essmann F, Schulze-Osthoff K, Journal of immunology 2013, 190, 4812.

[26]. Arango Duque G, Descoteaux A, Front Immunol 2014, 5, 491. [PubMed: 25339958]

[27]. Ryan DG, Murphy MP, Frezza C, Prag HA, Chouchani ET, O'Neill LA, Mills EL, Nature Metabolism 2018, 1, 16.

[28]. Sasikaran J, Ziemski M, Zadora PK, Fleig A, Berg IA, Nature chemical biology 2014, 10, 371. [PubMed: 24657929]

[29]. a)Ahn S, Jung J, Jang IA, Madsen EL, Park W, The Journal of biological chemistry 2016, 291, 11928; [PubMed: 27036942] b)Bergman JM, Wrande M, Hughes D, PLoS One 2014, 9, e109255; [PubMed: 25275605] c)Dolan SK, Welch M, Annual Review of Microbiology 2018, 72, 309;d)Lindsey TL, Hagins JM, Sokol PA, Silo-Suh LA, Microbiology 2008, 154, 1616. [PubMed: 18524916]

[30]. Teo AJT, Mishra A, Park I, Kim Y-J, Park W-T, Yoon Y-J, ACS Biomaterials Science & Engineering 2016, 2, 454. [PubMed: 33465850]

[31]. Schmalzried TP, Callaghan JJ, JBJS 1999, 81, 115.

[32]. Sadtler K, Singh A, Wolf MT, Wang X, Pardoll DM, Elisseeff JH, Nature Reviews Materials 2016, 1.

[33]. a)Huebsch N, Mooney DJ, Nature 2009, 462, 426; [PubMed: 19940912] b)Langer R, Tirrell DA, Nature 2004, 428, 487; [PubMed: 15057821] c)Mandla S, Davenport Huyer L, Wang Y, Radisic M, ACS Biomaterials Science & Engineering 2019, 5, 4542. [PubMed: 33455163]

[34]. Anderson JM, Rodriguez A, Chang DT, Seminars in immunology 2008, 20, 86. [PubMed: 18162407]

[35]. Chen Z, Bozec A, Ramming A, Schett G, Nat Rev Rheumatol 2018, DOI: 10.1038/s41584-018-0109-2.

[36]. Marim FM, Silveira TN, Lima DS Jr., Zamboni DS, PLoS One 2010, 5, e15263. [PubMed: 21179419]

[37]. Nemr K, Muller JEN, Joo JC, Gawand P, Choudhary R, Mendonca B, Lu S, Yu X, Yakunin AF, Mahadevan R, Metab Eng 2018, 48, 13. [PubMed: 29753069]

[38]. Causey T, Zhou S, Shanmugam K, Ingram L, Proceedings of the National Academy of Sciences 2003, 100, 825.

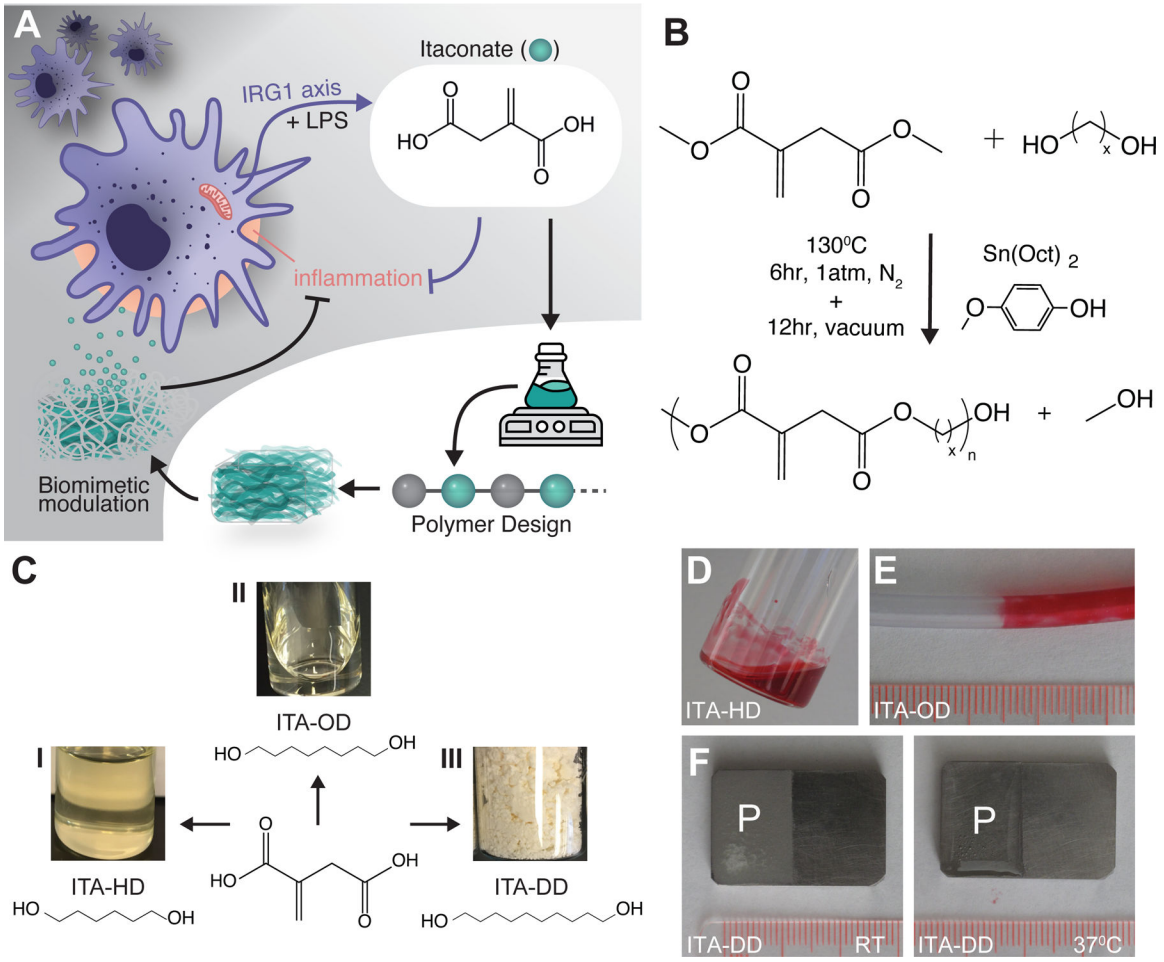

Fig. 1. Synthesis and processing of ITA containing polymers.

(**A**) A biomimetic approach to material design, harnessing ITA in degradable polyester materials for modulation of inflammation and infection upon degradation (purple arrows: cellular signaling pathways, black arrows: biomimetic material mechanisms) (**B**) General synthesis scheme for an ITA containing polyester using DMI with alcohols under a radical inhibitor and tin based catalyst. (**C**) Synthesis of ITA polyesters with (I) HD (II) OD, or (III) DD results in viscous liquids or a solid. (**D-F**) Demonstrated coating of ITA materials on common medical devices surfaces. (**D**) ITA-HD was visualized with soluble Sudan Red, and (**E**) similarly prepared ITA-OD was coated onto PVC tubing (ID: 1/8”, OD: 3/16”). (**F**) ITA-DD was solvent cast onto the surface of medical grade titanium alloy as a solid (room temperature), becoming a liquid at a physiologically relevant temperature (37°C). Scale: 1mm per notch, P indicates polymer coating.

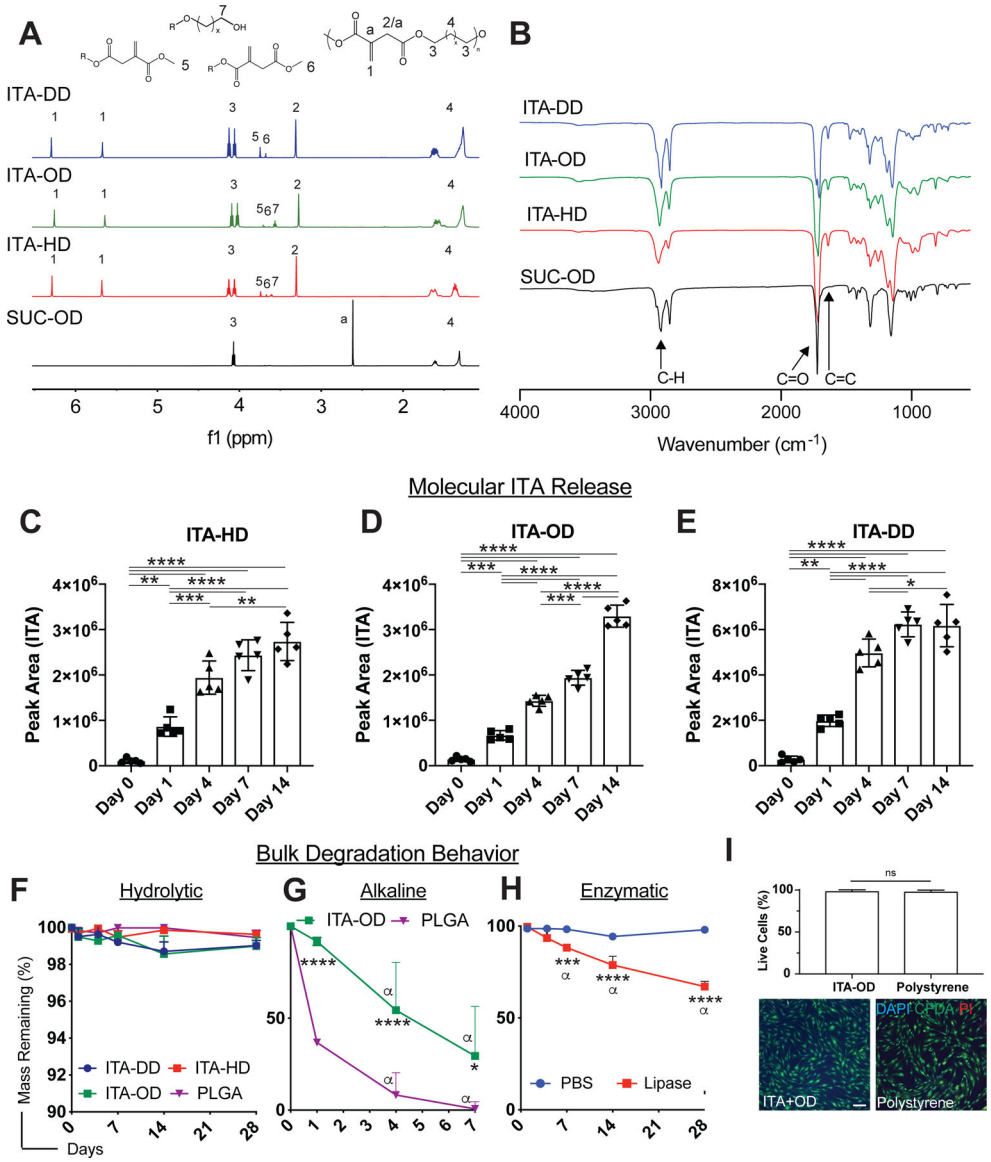

Fig. 2. High purity polymer materials harness the power of ITA

(**A-B**) Characterization of polymer purity and structure. Representative (**A**)^{1}H NMR and (**B**) FTIR spectra for ITA-DD (blue) and ITA-OD (green), ITA-HD (red) and SUC-OD (black) polyester. (**C-E**) Quantified ITA molecular release from material backbones. Integrated peak area for ITA presence in hydrolytic degradation supernatant extracts for (**C**) ITA-HD, (**D**) ITA-OD, and (**E**) ITA-DD. Data are mean ± SD, n=4. One way ANOVA followed by pairwise comparison with Tukey's multiple comparisons test. (**F-H**) Bulk degradation behavior of ITA polymers. (**F**) Hydrolytic degradation of ITA containing polyesters compared to PLGA in deionized distilled water over 28 days presents bulk stability. (**G-H**) Assessment of degradation under accelerated conditions; (**G**) ITA+OD and PLGA under alkaline conditions (1M) and (**H**) ITA+DD in the presence of lipase, indicate the ability for significant material dissolution over time. Two way ANOVA followed by pairwise comparison with Tukey's multiple comparisons test. α indicates significant difference

($p<0.05$) from day 1 within material group, other significance indicates comparison between ITA polyesters and control material at the same timepoint. (**I**) *In vitro* biocompatibility of ITA materials. Culture of dermal fibroblasts on ITA-OD presents similar cellular behavior to polystyrene controls (2 d post-seeding), quantified through image analysis 2 d post-seeding. Green: CFSA-SE (Live Cells), Red: PI (dead cells), Blue: DAPI (cell nuclei). Scale bars: 150μm. Data are mean ± SD, n=6. Student t-test. Statistical significance is indicated as *$p<0.05$ ** $p<0.01$, *** $p<0.001$, **** $p<0.0001$, ns=non-significant.

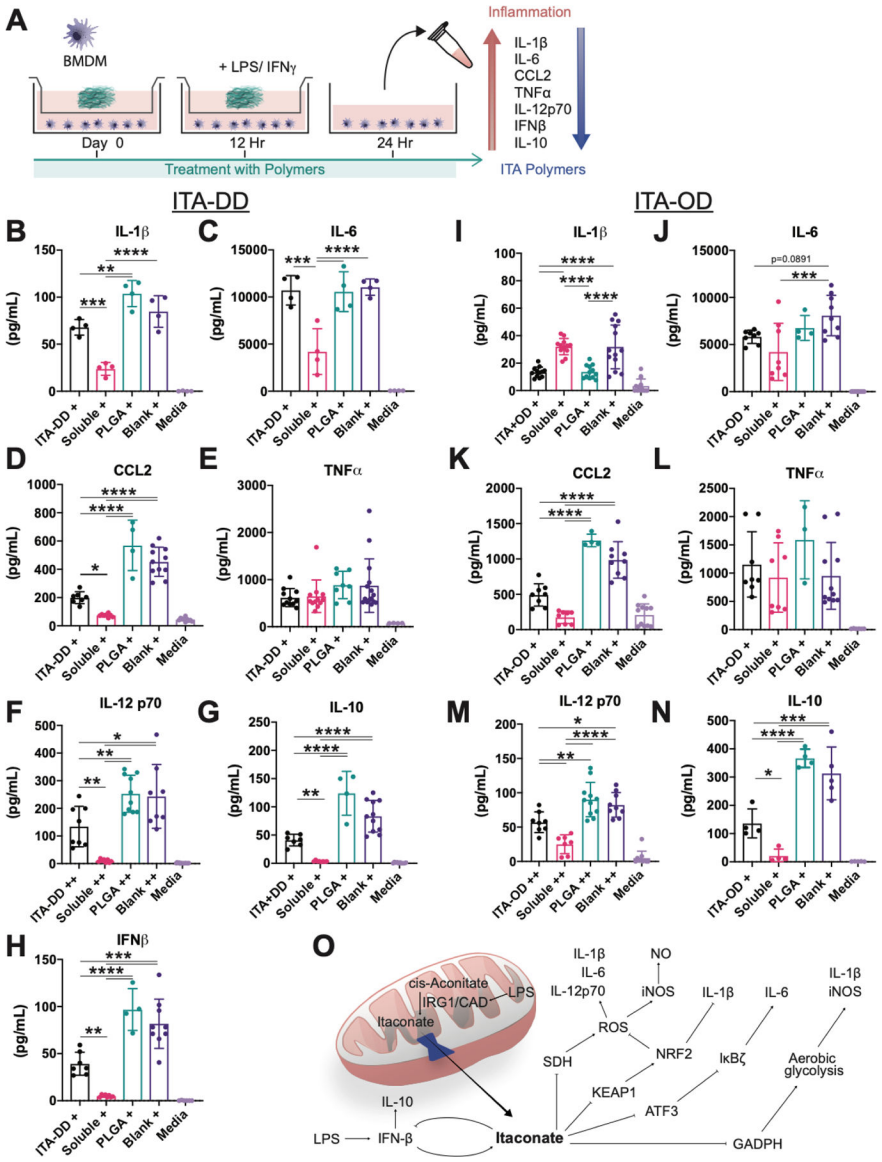

Fig. 3. New polymers recapitulate the mechanistic modulation of inflammatory cytokine behavior of small molecule ITA.

(**A**) Experimental schematic for the generation and assessment of polymer immunomodulation behavior with murine bone marrow derived macrophages *in vitro*. (**B-M**) Inflammatory cytokine quantification for key markers in innate immunity. Culture with (**B-H**) ITA-DD, (**I-N**) ITA-OD and soluble DMI demonstrated a mechanistically consistent downregulation of (**B, I**) IL-1β, (**C, J**) IL-6, (**D, K**) CCL2, (**F, M**) IL-12 p70, (**G, N**) IL-10, and (**H**) IFNβ, with (**E, L**) maintenance of TNFα expression when compared to PLGA inserts and insert free controls. + indicates stimulation with LPS (100 ng mL^{-1}), ++ indicates stimulation with LPS (100 ng mL^{-1}) and IFNγ (50 ng mL^{-1}). Data are mean ± SD, n≥4. One way ANOVA followed by pairwise comparison with Tukey's multiple comparisons test. Statistical significance is indicated as *p<0.05 ** p<0.01, *** p<0.001, **** p<0.0001. (**O**) Summary of previously proposed mechanisms of ITA based immunomodulation.

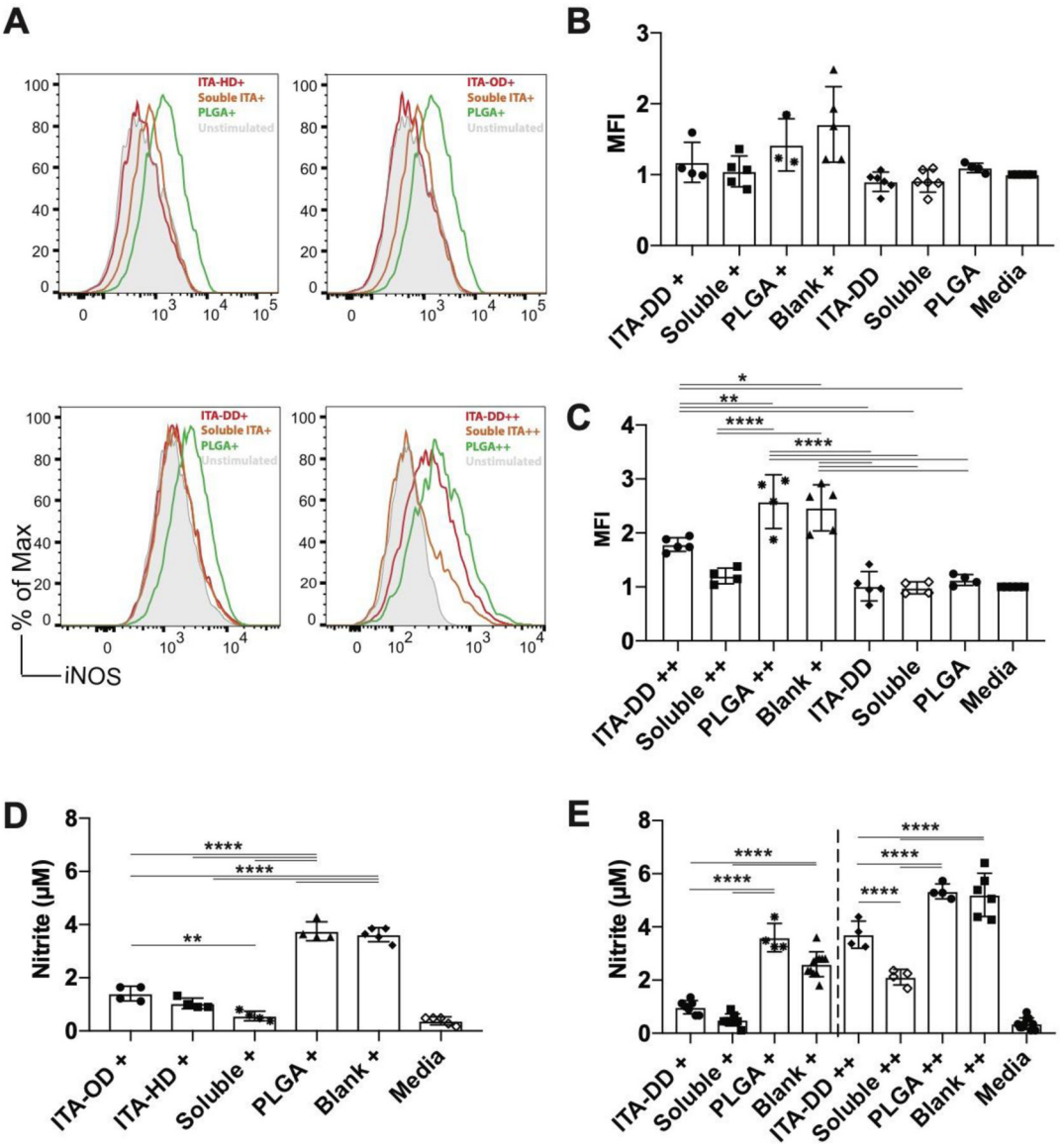

Fig. 4. New polymers reduce phenotypic nitric oxide based inflammation.

(**A**) Representative histogram of fluorescence indicating expression of NOS2 in response to stimulation (LPS or LPS/IFN**γ**) in cells treated with ITA-HD, ITA-OD, ITA-DD, soluble DMI, or PLGA with an unstimulated reference. (**B-C**) Quantified median fluorescence intensity for NOS2 expression for cells treated (12hr) with ITA-DD materials and stimulated with (**B**) LPS (100 ng mL^{-1}) or (**C**) LPS (100 ng mL^{-1}) and IFN**γ** (50 ng mL^{-1}) for 12 hr. (**D-E**) Supernatant nitrite content for (**D**) viscous liquid materials (ITA-HD, ITA-OD) stimulated with LPS and (**E**) ITA-DD stimulated with LPS (left) or LPS and IFN**γ** (right). + indicates stimulation with LPS (100 ng mL^{-1}), ++ indicates stimulation with LPS (100 ng mL^{-1}) and IFN**γ** (50n ng mL^{-1}). Data are (B-C) median ± SD, n≥3, (D-E) mean ± SD, n≥4. One way ANOVA followed by pairwise comparison with Tukey's multiple comparisons test. Statistical significance is indicated as *p<0.05 ** p<0.01, *** p<0.001, **** p<0.0001.

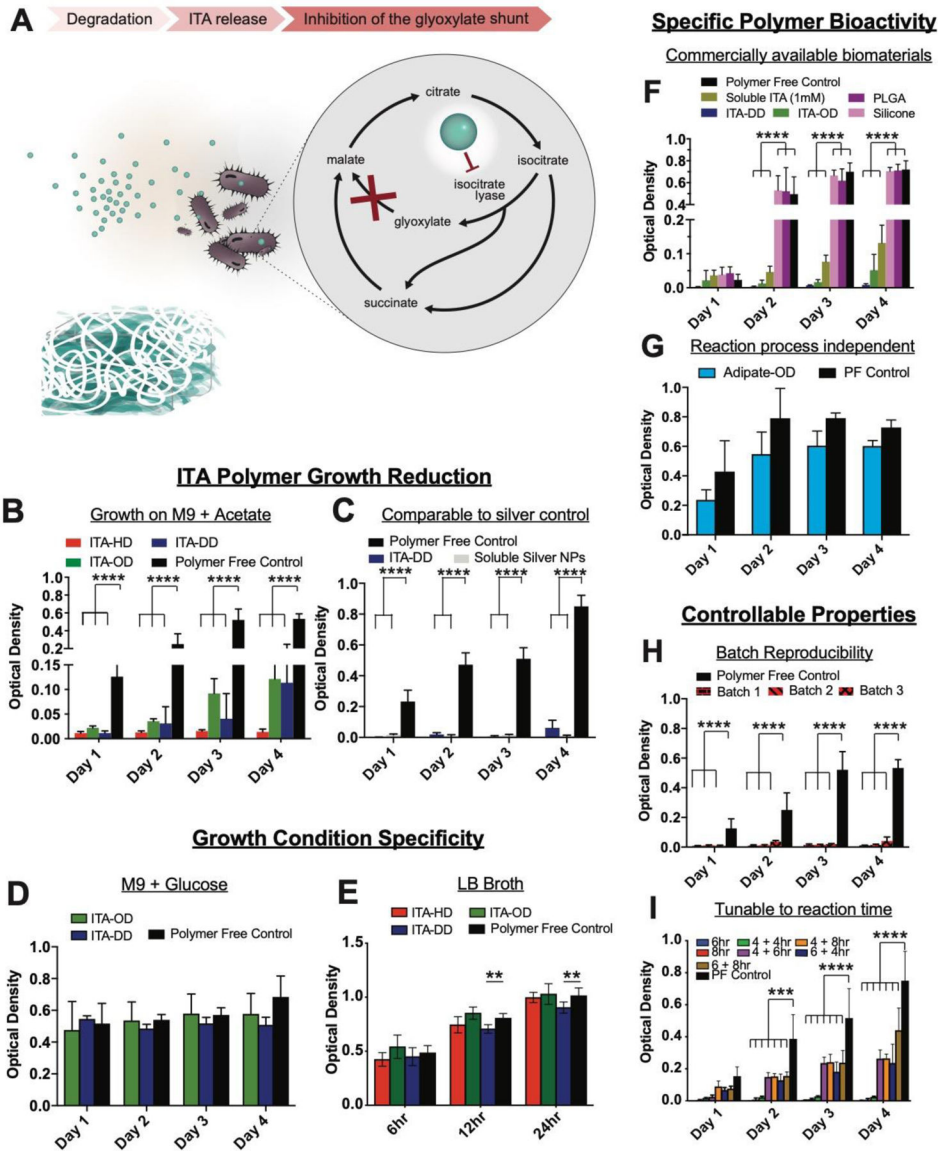

Fig. 5. ITA specific polymer bioactivity is demonstrated through mechanistic regulation of bacterial growth.

(**A**) Mechanism of ITA material bacterial growth modulation. ITA is a potent enzyme inhibitor of ICL, a key step in a glyoxylate growth cycle that allows for bacterial persistence on acetate growth substrates. (**B-I**) Suspension culture of *E. coli* in contact with polymer materials in M9 medium with acetate. (**B**) ITA-HD, ITA-OD, and ITA-DD present growth reduction on acetate in comparison to a polymer-free growth control, and (**C**) ITA-DD exhibited a similar effectiveness in bacterial growth inhibition as silver nanoparticles. (**D-E**) The regulatory behavior of ITA polymers was growth condition specific. (**D**) Culture with a glucose source and (**E**) LB broth indicated no appreciable inhibition. (**F-I**) Observed polymer bioactivity in M9 with acetate is specific to ITA polyesters. (**F**) ITA-OD and ITA-DD enabled significant bacterial growth reduction in a comparable fashion of soluble ITA (1 mM) whereas commercially available PLGA degradable polyester and viscous liquid silicone did not, and (**G**) inhibition was not observed with substitution of ITA with adipate in

the synthesis method. PF-polymer free control. (**H**) Inhibition behavior of ITA-HD on acetate growth substrate remained consistent across multiple synthesis batches, and (**I**) was tunable across a range of ITA+DD synthesis times (x +y hr indicates x: time at 1atm, y: time at vacuum pressure), with more pronounced inhibition at lower reaction times. Data are mean ± SD, n≥3. Two way ANOVA followed by pairwise comparison with Tukey's multiple comparisons test. Statistical significance is indicated as *p<0.05 ** p<0.01, *** p<0.001, **** p<0.0001.

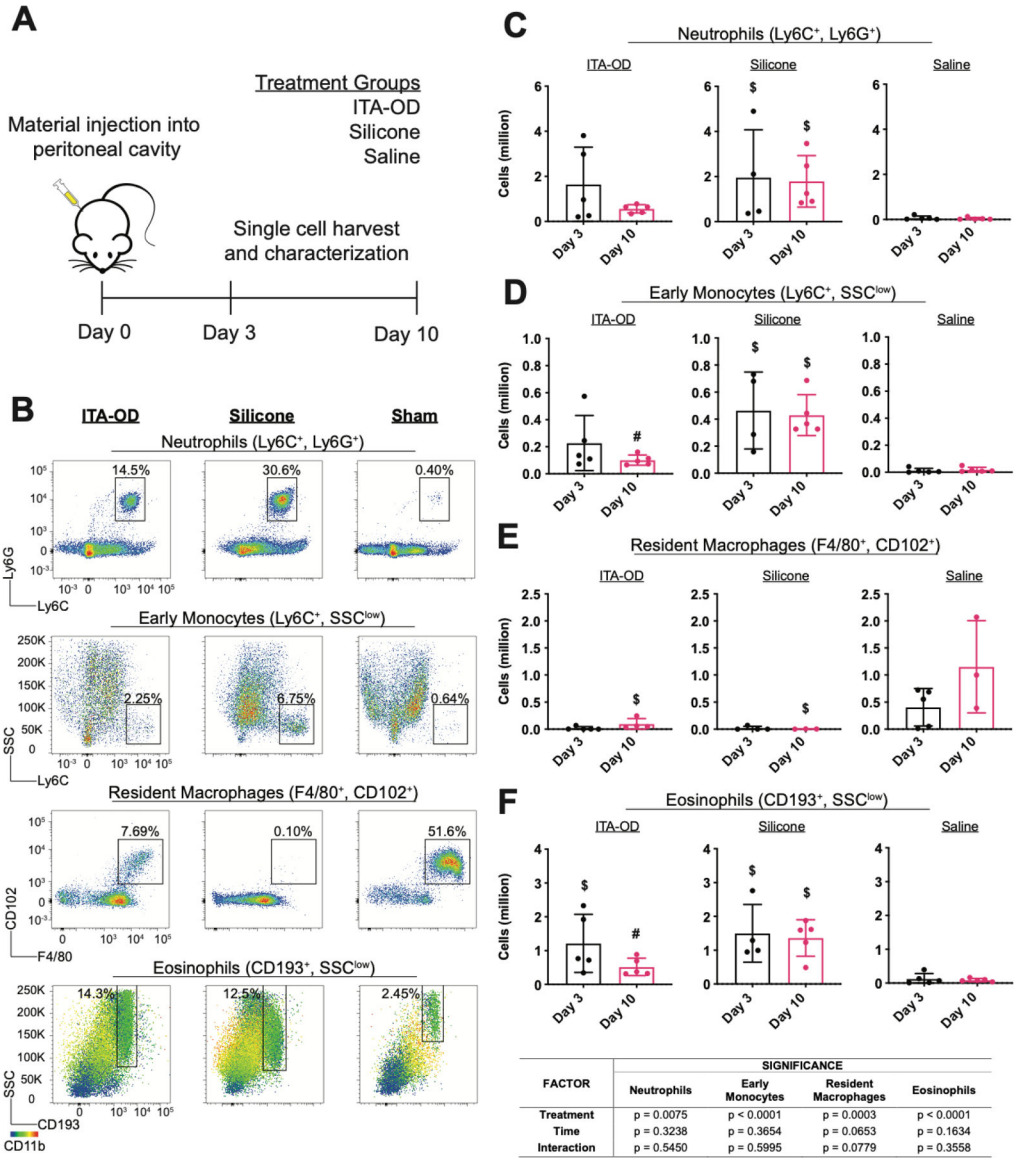

FACTOR	SIGNIFICANCE			
	Neutrophils	Early Monocytes	Resident Macrophages	Eosinophils
Treatment	p = 0.0075	p < 0.0001	p = 0.0003	p < 0.0001
Time	p = 0.3238	p = 0.3654	p = 0.0653	p = 0.1634
Interaction	p = 0.5450	p = 0.5995	p = 0.0779	p = 0.3558

Fig. 6. Injectable ITA polymer reduces biomaterial host response in a peritoneal infiltration model.

(**A**) Experimental schematic for peritoneal biomaterial associated immune cell infiltration model. (**B-F**) Using flow cytometry assessment, we quantified immune cell infiltration into the peritoneum following injection of ITA-OD (50μL), hydroxy terminated polydimethylsiloxane (Silicone) (50μL), or saline (Sham), with a comparable untreated group (Blank). (**B**) Representative flow cytometry plots for ITA-OD (left), silicone (center), and saline sham (right) ten days post injection. Percentage of total live cell populations is indicated for each identified cell population. Quantified cell populations (**C-F**) three and ten days post injection demonstrate the resolution of inflammatory infiltrate in ITA-OD treated animals. At each timepoint, we quantified (**C**) neutrophil, (**D**) early monocyte, (**E**) resident macrophage and (**F**) eosinophil populations. Cell population was determined through quantified total live cells and corresponding gated cell populations. Data are mean ± SD, n≥3. Two way ANOVA followed by pairwise comparison with Tukey's multiple

comparisons test. Statistical significance between material groups at each time point ($p<0.05$) is indicated as #: difference between polymer groups, $: difference from saline group.